Published in Eruptive Solar Flares
ed. Z. Svestka, B.V. Jackson,
M.E. Machado
(Springer-Verlag: Berlin), p. 69 (1992)

TRIGGERING OF ERUPTIVE FLARES: DESTABILIZATION OF THE PREFLARE MAGNETIC FIELD CONFIGURATION

Ronald L. Moore
NASA Marshall Space Flight Center, Space Science Laboratory
Huntsville, AL 35812, U.S.A.

George Roumeliotis
Stanford University, Center for Space Science & Astrophysics, ERL 306
Stanford, CA 94305, U.S.A.

ABSTRACT

This paper takes the three-dimensional configuration of the magnetic field in and before eruptive flares as our main guide to how the preflare field comes to lose its stability and erupt. From observed characteristics (1) of the preflare magnetic field configuration, (2) of the onset and development of the eruption of this configuration before and during the flare, and (3) of the onset and development of the flare energy release (i.e., the heating and particle acceleration) within the erupting field, the typical erupting field configuration for two-ribbon eruptive flares is constructed. The observational centerpiece for this construction is the evidence from the Marshall Space Flight Center vector magnetograph that strong magnetic shear along the main magnetic inversion line is critical for large eruptive flares. From (a) the empirical field configuration and (b) the observation that the initial flare brightening typically stems from points where opposite-polarity flux is gradually merging and canceling at or near the main inversion line, it is argued (1) that eruptive flares are driven by the eruptive expansion of the strongly sheared core of the preflare magnetic field, (2) that this eruption is triggered by preflare slow reconnection accompanying flux cancellation in the sheared core, and (3) that in some flares the triggering reconnection and flux cancellation is between opposite-polarity strands of the extant preflare sheared core field, while in other flares it is between the sheared core field and new emerging flux.

1. INTRODUCTION

Every solar flare is either "ejective" or "confined," i.e., either does or does not produce a coronal mass ejection (Machado et al. 1988). We think that most flares, whether ejective or confined, are appropriately termed "eruptive," because we think that most flares are driven by the same kind of global eruptive instability of the magnetic field (Moore et al. 1984; Sturrock et al. 1984; Kahler et al. 1988; Moore 1988a,b, 1990). However, the "eruptive solar flares" in the title of this Colloquium are a certain type of ejective flare. Accordingly, this paper explicitly considers only "ejective" eruptive flares, although the observations and ideas about the triggering and onset of these flares probably apply just as well to "confined" eruptive flares. Moreover, while flares often involve two or more impacted, interacting bipoles (Machado et al. 1988), here we will consider only eruptive flares that occur in single-bipole field configurations, i.e., flares that involve only one major magnetic inversion line. Ejective flares of this restricted class are the two-ribbon eruptive flares that are the topic of this Colloquium.

The purpose of this paper is to give the observational basis for the present "establishment" picture of two-ribbon eruptive flares and, from that, to infer how eruptive flares are triggered. Because of the limit on the length of this paper, no actual observations are shown. Instead, with reference to representative example observations in the literature, the key findings for the magnetic field configuration, its eruption, and the onset and development of the flare in this erupting field are shown in cartoons. From these empirical results, the eruptive global magnetic instability for these flares is inferred. From the global instability, together with observed features of the flare onset, comes the idea for the trigger, which is described with further cartoons. The inferred triggering process is slow reconnection accompanying gradual flux cancellation preceding the flare onset.

2. TYPICAL MAGNETIC FIELD CONFIGURATION BEFORE AND DURING ERUPTIVE FLARES

The typical three-dimensional form of the magnetic field before a two-ribbon eruptive flare is sketched on the left side of Figure 1 (Hirayama 1974; Heyvaerts, Priest, and Rust 1977; Moore and LaBonte 1980; Hagyard, Moore, and Emslie 1984; Sturrock et al. 1984; Moore et al. 1991). The field in the core of the bipole, i.e., the field rooted near the photospheric inversion line, is strongly sheared: these field lines closely trace the inversion line instead of going right across it as they would if the field had no shear, as would be the case if the field were in a current-free potential configuration. The shear in the bipole decreases with distance from the inversion line so that the strongly sheared core field is embedded in an arcade envelope of less-sheared closed magnetic field. Thus, the shear in the preflare bipole is markedly concentrated in a core channel running low along the inversion line.

Chromospheric images have long provided morphological evidence for the sheared core field at sites of eruptive flares. Before the flare, the photospheric magnetic inversion line is usually seen to be traced in the chromosphere by a dark filament (for example see the magnetograms and preflare Hα filtergrams for the famous [Skylab] eruptive flare of 29 July 1973 [Moore and LaBonte 1980] and for the famous [SMM] eruptive flare of 21 May 1980 [Hoyng et al. 1981]). The filament as a whole and the fibril substructure in the filament and in a channel somewhat wider than the filament (see Figure 7.6 of Martres and Bruzek [1977] and Figure 1 of Moore and Rabin [1985]) closely follow the direction of the inversion line; this is clear evidence that the field near the inversion line runs along it and hence is strong-

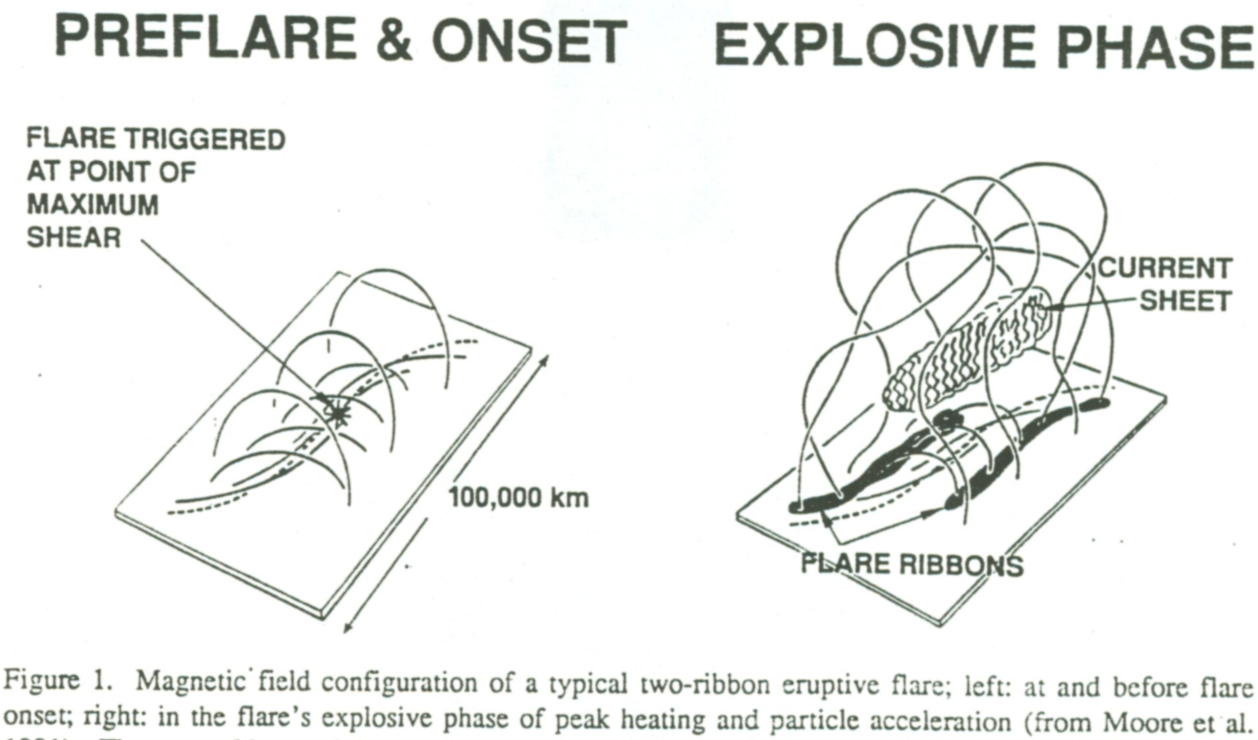

Figure 1. Magnetic field configuration of a typical two-ribbon eruptive flare; left: at and before flare onset; right: in the flare's explosive phase of peak heating and particle acceleration (from Moore et al. 1991). The core of lowest-lying strongest-sheared field shown in the preflare configuration is typically marked by a dark chromospheric filament; this provides a tracer showing that the core field begins to erupt before the explosive phase. By the peak of the explosive phase, the erupting core has greatly distended the envelope of the bipole, allowing the legs of the envelope arcade to collapse together beneath the erupted core (the double helix in this drawing) to form the current sheet and drive the heating and particle acceleration.

ly sheared (Foukal 1971). This qualitative chromospheric evidence for the core of sheared field in the preflare bipole has been confirmed and quantified by photospheric vector magnetograms. These data show that whenever (1) the field at the inversion line points along the inversion line to within 20 degrees and (2) such close alignment extends for about 10,000 km or more along the inversion line, then a large eruptive flare usually happens within a day; the first opposite points of the two chromospheric flare ribbons usually closely bracket the point of maximum shear. The vector magnetograms also confirm that the shear decreases with distance from the inversion line; the preflare photospheric field is closely aligned with the inversion line only in a channel that is roughly centered on the inversion line and that is about as wide as the overlying chromospheric filament and/or filament channel. For typical examples of these findings from vector magnetograms see Moore, Hagyard, and Davis (1987); Hagyard (1990); Hagyard, Venkatakrishnan, and Smith (1990); and Moore et al. (1991).

Soft X-ray and EUV coronal images provide further evidence that the preflare sheared core field lies within a closed-field envelope that is much less sheared than the core. Full-disk magnetograms show that most active regions are grossly bipolar: they have one main inversion line. Whether or not the bipole's core along the main inversion line is sheared enough to be marked by a chromospheric filament, coronal images show that the envelope of the bipole, the thick arcade of magnetic loops rooted well away from the core, has little shear, i.e., the envelope of coronal magnetic loops looks pretty much like a potential field (for examples of magnetograms together with coronal images showing the non-twisted, potential character of the envelope field in active regions, see Sheeley [1981] and Moore [1990]). From these observations we might expect that the envelope field still has little shear just before an eruptive flare. This expectation has been verified by a few preflare coronal images of the sites of eruptive flares (for two examples, see Moore and LaBonte [1980] and Kahler, Webb, and Moore [1981]).

Once a two-ribbon eruptive flare begins, the explosive phase of flare energy release (the phase of most powerful and most impulsive plasma heating and particle acceleration) usually ensues within several minutes and peaks within a few more minutes. The typical configuration of the magnetic field and flare at the peak of the explosive phase is sketched on the right side of Figure 1 (Hirayama 1974; Heyvaerts, Priest, and Rust 1977; Moore and LaBonte1980; Hagyard, Moore, and Emslie 1984; Sturrock et al. 1984; Moore et al. 1991). By this time in the flare, some of the sheared core field has erupted up, stretching the legs of the envelope arcade. The two chromospheric flare ribbons have formed near the inversion line and are rapidly spreading away. Hot coronal flare loops straddling the inversion line and rooted in the ribbons are being formed by reconnection at the current sheet between the two merging legs of the stretched envelope. The erupting core field often carries much of the preflare chromospheric filament with it (Tang 1986); the core eruption can thereby be traced in chromospheric movies. These movies show that by the peak of the explosive phase, in the manner of the erupting double helix in our explosive-phase cartoon in Figure 1, the erupting core field typically has arched up to a height of several times the height of the preflare filament. For example, see the filament eruption in the OSO-7 flare of 10 October 1971 shown in Roy and Tang (1975) and in Moore (1987). Other good examples are shown in Kahler et al. (1988).

3. TYPICAL ONSETS OF ERUPTIVE FLARES

This paper is intended to focus on the triggering of eruptive flares: How does the preflare field configuration lose its equilibrium so that it erupts and changes into the transient configuration of the explosive phase? For observational clues to this question, the obvious things to look at are the onset of the core eruption and the initial flare brightenings.

Most onsets of eruptive flares are covered by the following three cases: onset in the absence of emerging flux, onset with localized emerging flux (a small emerging bipole) on the main inversion line, and onset with localized emerging flux off the main inversion line but still under the envelope of the preflare bipole. In Figure 2, the configuration of the magnetic field and initial flare ribbons is shown for each of these three cases at the onset of flare brightening. The core eruption traced by the filament usually begins somewhat before any noticeable flare brightening. This early stage of the eruption at

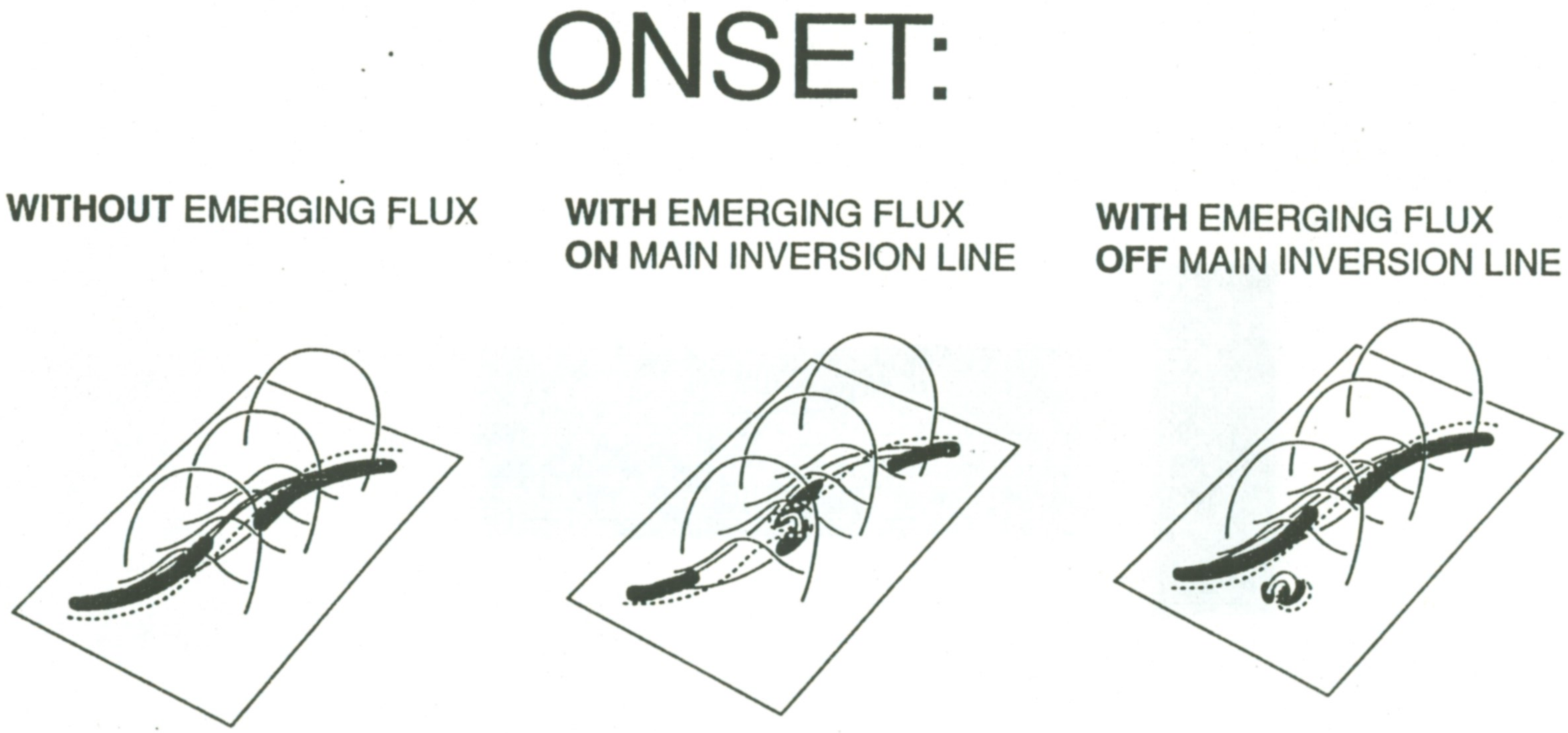

Figure 2. Typical onsets of eruptive flares; left: no emerging flux; center: emerging flux on main inversion line; right: emerging flux off main inversion line. Here, as in Figure 1, the dashed lines are magnetic inversion lines, dividing areas of opposite polarity in the photosphere; black areas are ribbons of chromospheric flare brightening. In all three cases, at flare-ribbon onset the sheared core field along and above the main inversion line has begun to erupt upward, distending the surrounding envelope field, and the initial flare ribbons along the main inversion line are tucked under the erupting core.

brightening onset is indicated in Figure 2 by the moderate upward arching and bulging of the core field in comparison to the core field in the preflare configuration in Figure 1. In the case of no emerging flux, the initial flare brightening is close against the inversion line under the erupting core. In the case of emerging flux on the main inversion line, the initial brightening is again all very near the inversion line under the erupting core; in this case, some of the initial brightening is at the place on the main inversion line where the little bipole is emerging. When the small emerging bipole in off the main inversion line, some of the initial brightening is at that location, but most of it is right along the inversion line under the erupting core. Thus, when emerging flux is present, it is usually involved in the flare onset, but with or without emerging flux, an eruptive flare begins with brightening close along the inversion line under the sheared core field that is starting to erupt.

A good example of an eruptive flare that happened without emerging flux is the SMM flare of 25 June 1980; its onset is shown in Figure 5 of Kahler et al. (1988). The preflare magnetic field configuration and evolution at this flare site was examined in detail in high-resolution images by Gaizauskas (Hagyard et al. 1986): there was no sign of emerging flux near the onset of this flare. Another eruptive flare with no noticeable emerging flux is the large SMM flare of 24/25 April 1984. For the preflare vector magnetogram and onset of this flare, see Hagyard, Venkatakrishnan, and Smith (1990) and Hagyard (1990). A good example of an eruptive flare with emerging flux on the inversion line is the SMM flare of 21 May 1980. For magnetograms showing the emerging flux, see Harvey (1983); for the flare onset (in soft X-ray emission) see Batchelor and Hindsley (1991) or Moore et al. (1991). The initial brightening in soft X-rays was a long stripe that traced the inversion line and that was brightest at the site of emerging flux (the X-ray emitting plasma was apparently on field lines rooted along the inversion line, like the field lines rooted in the flare ribbons in Figure 2). The Skylab flare of 29 July 1973 might be another example of an eruptive flare with emerging flux on its main inversion line. There was a small bipole on the inversion line at the time of the flare, but in high-resolution Hα filtergrams it did not look like an emerging bipole. More likely, it was two clumps of opposite polarity flux merging and canceling at the main inversion line. Hence, this flare is probably another example of an eruptive flare without emerging flux. In any case, after the preflare filament began to erupt, the flare ribbons turned on closely bracketing the the small bipole and then rapidly extended closely along the inversion line to attain a configuration like the flare ribbons in Figure 2. For the magnetogram and onset of this flare, see Moore and LaBonte (1981) and Moore, Horwitz, and Green (1984). Finally, a good example of an eruptive flare onset involving emerging flux off the main inversion line is that of the flare of 10 April 1980 shown in Moore et al. (1984).

4. INFERRED GLOBAL LOSS OF STABILITY FOR ERUPTIVE FLARES

Before using the observed characteristics of the onsets of eruptive flares to infer how eruptive flares are triggered, we will first infer - from the typical configuration of the field and flare before, during, and after flare onset - the overall instability that drives the field eruption and flare energy release. That is, our next step toward finding the trigger is to consider what instability is to be triggered.

The perspective sketches in the first three panels of Figure 3 reiterate our points about the preflare field configuration and the form of the erupting field and flare brightening within it during the onset and the explosive phase (= impulsive phase) of the flare energy release. The perspective sketch in the fourth panel of Figure 3 shows the configuration of the field and flare ribbons well after the explosive phase. These sketches suggest that an eruptive flare is basically a magnetic explosion that starts in the sheared core of the overall bipole. In the preflare state, because the magnetic pressure in active regions is much greater than the plasma pressure, the field is in an equilibrium configuration that is nearly force-free (e.g., Tandberg-Hanssen and Emslie 1988). That is, in the preflare configuration the pressure of the magnetic field (which tries to make the configuration explode) is confined by the tension of the magnetic field (e.g., Cowling 1957). Apparently, the global instability that results in the explosion that is an eruptive flare is a global loss of balance between the pressure and the tension: the configuration explodes when the field tension can no longer restrain the field pressure.

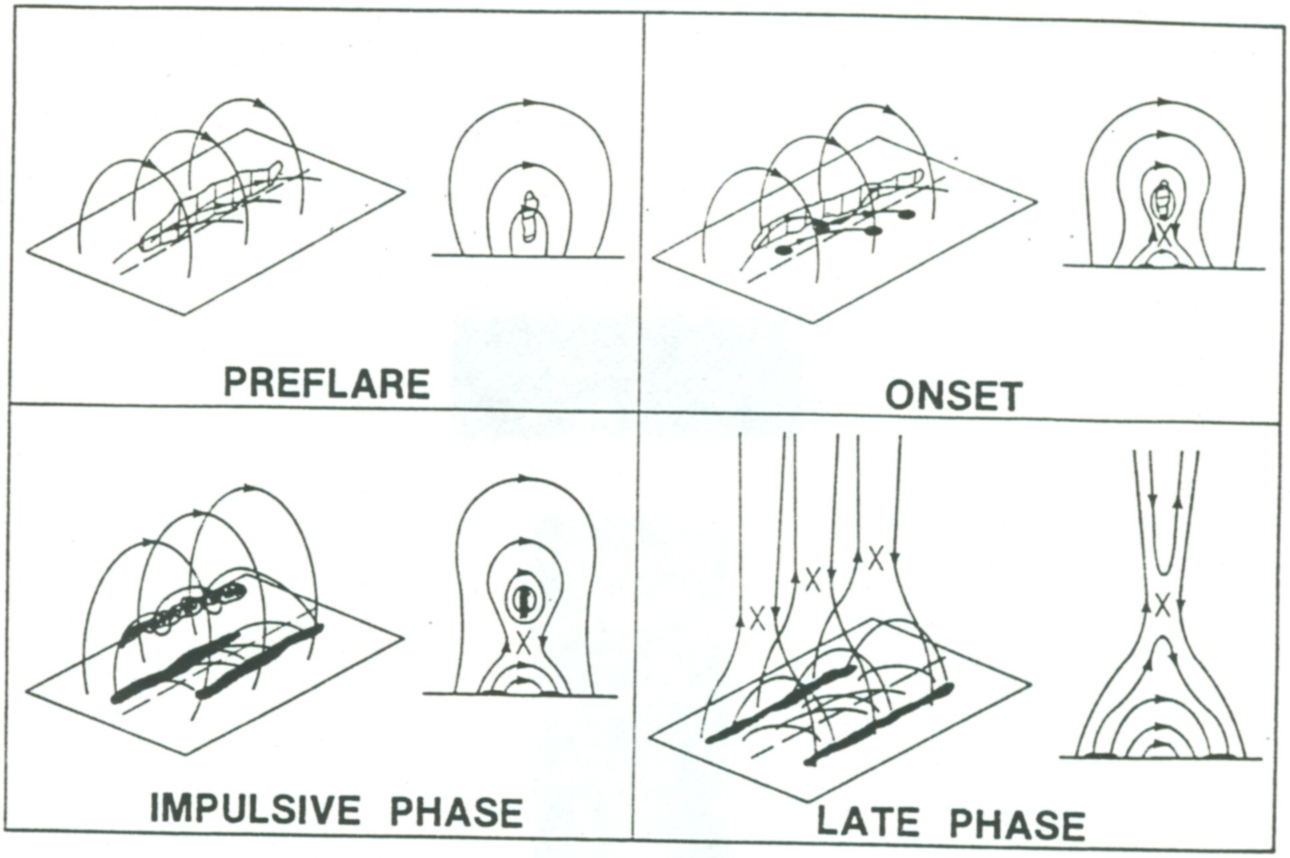

Figure 3. Progression of the field configuration, reconnection, and flare ribbons in a typical eruptive flare (from Hagyard, Moore, and Emslie 1984). In the preflare state (preflare panel), the field configuration is in force-free, magnetostatic, stable equilibrium, a balance between magnetic pressure and magnetic tension. Before the onset of flare heating (i.e., at some time after the preflare panel but before the onset panel), the core field loses its equilibrium: a loss of magnetic tension results in unbalanced magnetic pressure that causes the core field to begin to erupt. The distended field around the erupting core then collapses into the space that that the core has just vacated (onset panel); this forms a current sheet and drives fast reconnection, heating, and particle acceleration (onset, impulsive phase, and late phase panels). This reconnection further untethers the core field, providing a positive feedback that sustains the magnetic explosion (onset and impulsive phase panels). The whole process of coordinated eruption and reconnection is driven by the magnetic pressure of the unleashed core field.

The end-view sketches in Figure 3 show the reconnection that is inferred from the configuration of the field and flare ribbons and the progression of the core eruption and ribbon spreading. In the late phase, the reconnection recloses the envelope field that has been opened by the expulsion of the core field. The reconnection process supplies to the newly formed coronal loops the heat that makes them bright in soft X-ray emission and that makes their feet bright in chromospheric emission. Hence, the reconnection and flare energy release in the late phase is a consequence of the core eruption (Kopp and Pneuman 1976). As depicted in Figure 3, the reconnection in the late phase is the continuation of reconnection that begins with the onset of flare brightening. Thus, it is compatible with the observations to assume that all of the flare brightening, from its beginning, is powered through reconnection. Because the reconnection and flare energy release in the late phase seems quite obviously to be a consequence of the core eruption, and because the core eruption is already in progress at the onset of flare brightening, it is our view that all of the flare energy release and the reconnection inherent to the energy release (i.e., the reconnection depicted in Figure 3) from onset on are driven by the core eruption.

We call the reconnection depicted in Figure 3, "fast" reconnection because it has a fast driver, the core eruption. We take this fast reconnection above the inversion line to be a crucial part of the global instability that sustains the field explosion: by further unleashing the field it gives a positive feedback to the eruption (Moore and LaBonte 1981; Hagyard, Moore, and Emslie 1984; Moore, Horwitz, and Green 1984, Sturrock et al. 1984). Previous papers (e.g., Heyvaerts, Priest, and Rust 1977; Moore et al. 1991; and those papers cited in the preceding sentence) have suggested that the flare is triggered by the reconnection that accompanies the onset of flare brightening. In this paper, we depart from that view. It is our view that global stability of the field configuration is lost before onset of flare brightening and that the fast reconnection that gives this brightening is part of the global instability and is driven by the global instability; the fast reconnection at brightening onset is not the trigger of the flare, it is part of the flare. We thus conclude that the trigger must be something other than the onset of the fast reconnection; the trigger is something that happens earlier that renders the the configuration globally unstable to eruption.

5. INFERRED TRIGGER FOR ERUPTIVE FLARES: SLOW RECONNECTION

We are now ready to infer the trigger for eruptive flares. Our above discussion of the global instability that drives eruptive flares argues that the beginning of the core eruption is the beginning of the global instability. From this we infer that the trigger that we seek is the trigger of the core eruption. Our picture of the global instability also suggests that the core eruption is triggered when the magnetic pressure of the sheared core field can no longer be balanced by the magnetic tension. The tension is provided by the tying of the field to the photosphere. Hence, we infer that the triggering is the end result of a process that gradually erodes the core field's linkage to the photosphere until the confinement of the core field becomes untenable. The onset of flare brightening (which we think marks the onset of fast reconnection) is at magnetic inversion lines, often including inversion lines around emerging flux (as in Figure 2). All these considerations suggest (1) that the triggering process is located at the sites of initial flare brightening, and (2) that the triggering process is preflare gradual reconnection that accompanies preflare flux cancellation, as we will now discuss.

It is observed that when two patches of magnetic flux of opposite polarity are brought together by photospheric flows, flux cancells at the inversion line where the two patches meet (Martin and Livi, these proceedings). The cancellation is apparently accomplished by submergence of a succession of low magnetic loops formed from the merging opposite-polarity fields by reconnection at or above the photospheric inversion line (as in Figure 5 of Rabin, Moore, and Hagyard 1984). The typical sites of initial flare brightening in Figure 2 (at the inversion line in the sheared core and at inversion lines around emerging flux), are also typically sites of preflare flux cancellation (Martin and Livi, these proceedings). Cancellation reconnection is probably much slower than the reconnection in eruptive flares because its driver (photospheric flow; < 1 km/s) is much slower than the driver (core eruption; 10-100 km/s) of the reconnection in eruptive flares. Hence, we call the preflare cancellation reconnection "slow" reconnection. We think that this slow reconnection is the trigger for eruptive flares.

In Figure 4 we have sketched the operation of our proposed preflare process for triggering eruptive flares; the three cases shown correspond to the three typical cases of eruptive flare onset shown in Figure 2. In the case of no emerging flux, the triggering cancellation reconnection is on the main inversion line, in the sheared core. In this case, the core field that goes through the cancellation reconnection process loses half of its linkages to the photosphere, while its horizontal flux remains nearly unchanged. So, in this case, the flare is triggered by what may be called "tether cutting." This case of cancellation reconnection on the main inversion line has been modeled by van Ballegooijen and Martens (1989). In the case of emerging flux on the inversion line of the sheared core, the processed core field again loses half of its ties to the photosphere. So, this is again triggering by tether cutting, but driven by flux emergence rather than by photospheric flow converging on the main inversion line as required in the previous case. Finally, in the case of emerging flux off the inversion line of the core, the number of ties of the core field to the photosphere is not reduced, but the distance between the tie points is increased, which weakens the tension of the core field relative to its pressure. So, we term this process "tether weakening."

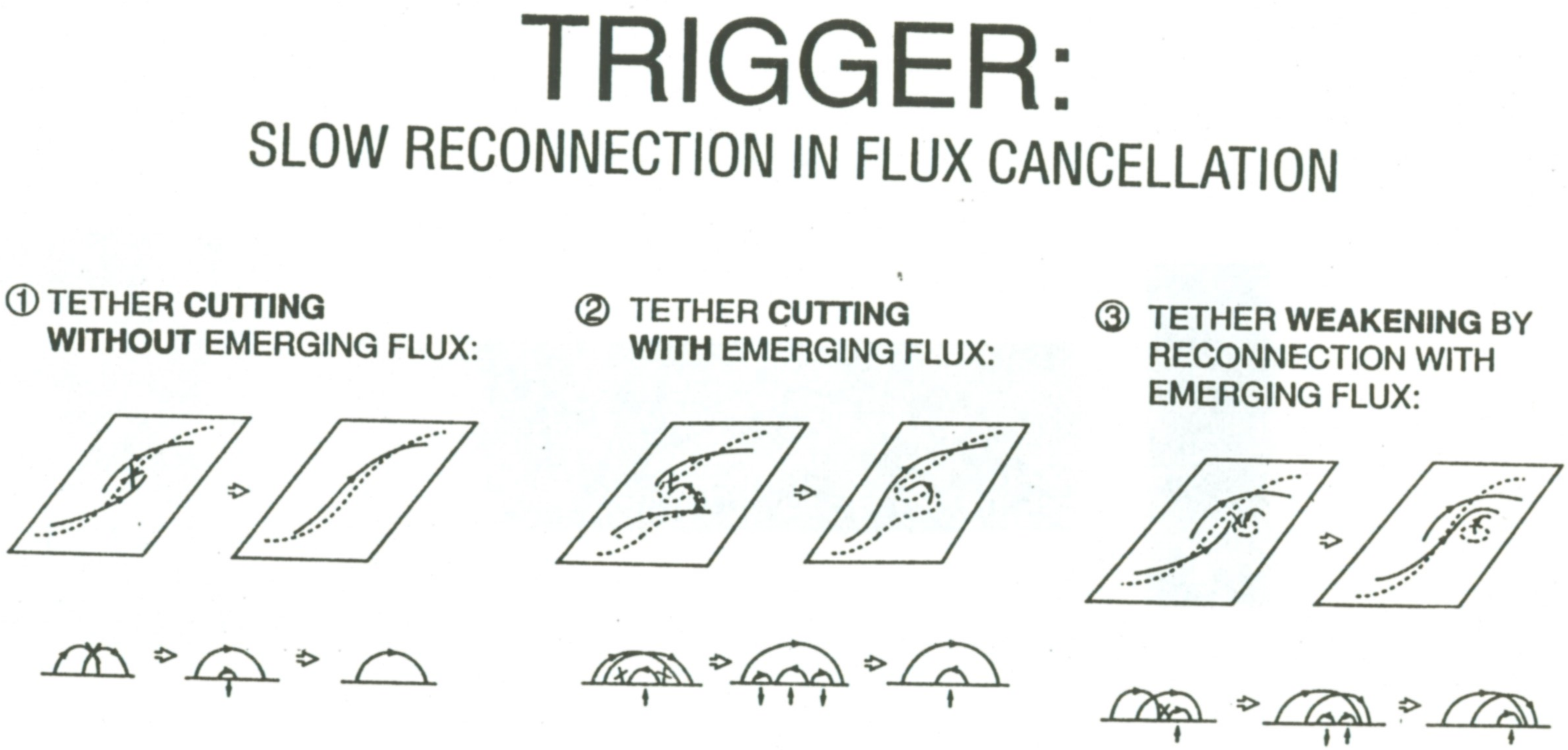

Figure 4. Inferred process for triggering typical onsets of eruptive flares; left: no emerging flux; center; emerging flux on main inversion line; right: emerging flux off main inversion line. The field lines shown are in the core of the preflare field configuration shown in Figures 1-3. The sequences of 2-D sketches below the perspective sketches show the reconnection, emergence, and submergence of field in an end view along the main inversion line. X's mark reconnection. Vertical arrows below the 2-D sketches mark flux emergence (upward arrow) and flux submergence (downward arrow).

In all cases, the preflare cancellation reconnection continues until the core field becomes so weakly tethered that it can begin to erupt and drive fast reconnection under it over the main inversion line. The trigger is that last bit of slow reconnection that renders the core field globally unstable to eruption and fast reconnection.

6. CLOSING

The main new idea of this paper is that eruptive flares are not triggered by the reconnection that happens with the initial flare brightening, but by slower reconnection that precedes the initial flare reconnection at the same sites. The flare reconnection is fast reconnection that is driven by and sustains the core eruption; the preflare triggering reconnection is much slower reconnection in flux cancellation driven by photospheric flows. We have tacitly assumed that the cancellation reconnection produces a much lower rate of magnetic energy dissipation than does the initial fast reconnection in the flare onset. Can our proposed preflare slow reconnection occur without producing more heating than observations allow? We are presently pursuing this question through a modeling study of slowly driven reconnection (Roumeliotis and Moore, in preparation).

ACKNOWLEDGEMENTS

This work was supported by NASA through the Solar Physics Branch of its Space Physics Division. The paper was improved by helpful advise from Marcos Machado. Ron Moore first heard of the idea that flares might be triggered by preflare slow reconnection in a talk given by Dan Spicer at Marshall Space Flight Center in 1985.

REFERENCES

Batchelor, D. A., and Hindsley, K. P. 1991, Solar Phys., **135**, 99.

Cowling, T. G. 1957, Magnetohydrodynamics (Interscience Publishers, Inc.: New York), p. 9.

Foukal, P. 1971, Solar Phys., **19**, 59.

Hagyard, M. J. 1990, Mem. Soc. Astron. It., **Vol. 61, No. 2**, p. 337.

Hagyard et al. 1986, in Energetic Phenomena on the Sun, ed. M. R. Kundu and B. Woodgate, NASA CP-2439 (NASA: Washington, D. C.), Ch. 1, p. 16.

Hagyard, M. J., Moore, R. L., and Emslie, A. G. 1984, Adv. Space Res., **Vol. 4, No. 7**, p. 71.

Hagyard, M. J., Venkatakrishnan, P., and Smith, J. B., Jr. 1990, Astrophys. J. Supp., **73**, 159.

Harvey, J. W. 1983, Adv. Space Res., **Vol. 2, No. 11**, p. 31.

Heyvaerts, J., Priest, E. R., and Rust, D. M. 1977, Astrophys. J., **216**, 123.

Hirayama, T. 1974, Solar Phys., **34**, 323.

Hoyng, P. et al. 1981, Astrophys. J. (Letters), **246**, L155.

Kahler, S. W., Moore, R. L., Kane, S. R., and Zirin, H. 1988, Astrophys. J., **328**, 824.

Kahler, S. W., Webb, D. F., and Moore, R. L. 1981, Solar Phys., **70**, 335.

Kopp, R. A., and Pnueman, G. W. 1976, Solar Phys., **50**, 85.

Machado, M. E., Moore, R. L., Hernandez, A. M., Rovira, M. G., Hagyard, M. J., and Smith, J. B., Jr. 1988, Astrophys. J., **326**, 425.

Martres, M. J., and Bruzek, A. 1977, in Illustrated Glossary for Solar and Solar-Terrestrial Physics, ed. A. Bruzek and C. J. Durrant (Reidel: Boston), Ch. 7, p. 53.

Moore, R. L. 1987, Solar Phys., **113**, 121.

Moore, R. L. 1988a, Astrophys. J., **324**, 1132.

Moore, R. L. 1988b, in Solar and Stellar Coronal Structure and Dynamics, ed. R. C. Altrock (National Solar Observatory: Sacramento Peak, Sunspot, New Mexico), p. 520.

Moore, R. L. 1990, Mem. Soc. Atron. It., **Vol. 61, No. 2**, p. 317.

Moore, R. L., Hagyard, M. J., and Davis, J. M. 1987, Solar Phys., **113**, 347.

Moore, R. L., Hagyard, M. J., Davis, J. M., and Porter, J. G. 1991, in Flare Physics in Solar Activity Maximum 22, ed. Y. Uchida, R. C. Canfield, T. Watanabe, and E. Hiei (Springer-Verlag: Berlin), p. 324.

Moore, R. L., Horwitz, J. L., and Green, J. L. 1984, Planet. Space Sci., **Vol. 32, No. 11**, p. 1439.

Moore, R. L., Hurford, G. J., Jones, H. P., and Kane, S. R. 1984, Astrophys. J., **276**, 379.

Moore, R. L., and LaBonte, B. J. 1980, in Solar and Interplanetary Dynamics, ed. M. Dryer and E. Tandberg-Hanssen (Reidel: Boston), p. 207.

Moore, R., and Rabin, D. 1985, Ann. Rev. Astron. Astrophys., **23**, 239.

Rabin, D., Moore, R., and Hagyard, M. J. 1984, Astrophys. J., **287**, 404.

Roy, J.-R., and Tang, F. 1975, Solar Phys., **42**, 425.

Sheeley, N. R., Jr. 1981, in Solar Active Regions, ed. F. Q. Orrall (Colo. Assoc. Univ. Press: Boulder), p. 17.

Sturrock, P. A., Kaufman, P., Moore, R. L., and Smith, D. F. 1984, Solar Phys., **94**, 341.

Tandberg-Hanssen, E., and Emslie, A. G. 1988, The Physics of Solar Flares (Cambridge University Press: Cambridge), p. 75.

Tang, F. 1986, Solar Phys., **105**, 399.

van Ballegooijen, A. A., and Martens, P. C. H. 1989, Astrophys. J., **343**, 971.